Absolute chlorine and hydrogen atom quantum yield measurements in the 193.3 nm photodissociation of CH_3CFCl_2 (HCFC-141b)

Almuth Läuter
Physikalisch-Chemisches Institut der Universität Heidelberg, Im Neuenheimer Feld 253, D-69120 Heidelberg, Germany

Dhanya Suresh
Radiation Chemistry and Chemical Dynamics Division, Bhabha Atomic Research Centre, Mumbai 400-085, India

Hans-Robert Volpp[a)]
Physikalisch-Chemisches Institut der Universität Heidelberg, Im Neuenheimer Feld 253, D-69120 Heidelberg, Germany

(Received 21 October 2002; accepted 16 January 2003)

The dynamics of chlorine and hydrogen atom formation in the 193.3 nm gas-phase laser photolysis of room-temperature 1,1-dichloro-1-fluoroethane, CH_3CFCl_2 (HCFC-141b), were studied by means of the pulsed-laser-photolysis and laser-induced fluorescence (LIF) ''pump-and-probe'' technique. Nascent ground-state $Cl(^2P_{3/2})$ and spin–orbit excited $Cl^*(^2P_{1/2})$ as well as $H(^2S)$ atom photofragments were detected under collision-free conditions by pulsed Doppler-resolved laser-induced fluorescence measurements employing narrow-band vacuum ultraviolet probe laser radiation, generated via resonant third-order sum-difference frequency conversion of dye laser radiation in krypton. Using HCl photolysis as a reference source of well-defined $Cl(^2P_{3/2})$, $Cl^*(^2P_{1/2})$, and H atom concentrations, values for the chlorine-atom spin–orbit branching ratio $[Cl^*]/[Cl]=0.36\pm0.08$, the total chlorine atom quantum yield ($\Phi_{Cl+Cl^*}=1.01\pm0.14$), and the H atom quantum yield ($\Phi_H=0.04\pm0.01$) were determined by means of a photolytic calibration method. From the measured Cl and Cl* atom Doppler profiles the mean relative translational energy of the chlorine fragments could be determined to be $E_{T(Cl)}=157\pm12$ kJ/mol and $E_{T(Cl^*)}=165\pm12$ kJ/mol. The corresponding average values 0.56 and 0.62 of the fraction of total available energy channeled into $CH_3CFCl+Cl/Cl^*$ product translational energy were found to lie between the limiting values 0.36 and 0.85 predicted by a soft impulsive and a rigid rotor model of the $CH_3CFCl_2\rightarrow CH_3CFCl+Cl/Cl^*$ dissociation processes, respectively. The measured total chlorine atom quantum yield along with the rather small H atom quantum yield as well as the observed energy disposal indicates that direct C–Cl bond cleavage is the most important primary fragmentation mechanism for CH_3CFCl_2 after photoexcitation in the first absorption band. © *2003 American Institute of Physics.* [DOI: 10.1063/1.1558316]

I. INTRODUCTION

CH_3CFCl_2 (hydrochlorofluorocarbon: HCFC-141b) has been widely utilized as a replacement for $CFCl_3$ (chlorofluorocarbon: CFC-11) in the manufacturing process of closed-cell insulating foams and for $CFCl_2CF_2Cl$ (CFC-113), which is used as a solvent in a variety of industrial processes.[1,2] As a consequence, measurements of tropospheric concentrations of this compound have shown a rapid increase since 1994.[3] Although its production has been stopped in 1996 and, based on the revised Montreal Protocol, its use will be phased out in developed countries by 2020,[4] the release into the atmosphere is expected to further increase in the coming few decades because of long-term uses of the previously manufactured products.[5] Despite the fact that HCFCs such as CH_3CFCl_2, which contain one or more C–H bonds, can be oxidized by OH radicals in the troposphere,[6] they still have the potential to lead to noticeable chlorine transportation to the stratosphere[7] where they can be decomposed via radical reactions or photolytically after UV photon absorption in the 230–190 nm spectral region.[8,9] As a consequence, a number of reaction kinetics studies of CH_3CFCl_2 with atmospherically important radicals such as OH,[10] $O(^1D)$,[11] and Cl,[12] along with studies on the UV photodissociation dynamics of CH_3CFCl_2, have been reported so far.[13,14]

In Ref. 13, ground-state $Cl(^2P_{3/2})$ and spin–orbit excited $Cl^*(^2P_{1/2})$ as well as $H(^2S)$ atom photofragment formation could be observed in the 193.3 nm photolysis of CH_3CFCl_2 and the relative product branching ratio $[H]/[Cl+Cl^*]$ along with the chlorine-atom spin–orbit branching ratio $[Cl^*]/[Cl]$ were reported. In further experiments, the influence of selective methyl stretching vibrational excitation on the Cl atom spin–orbit branching[14] and the H atom versus chlorine atom product branching[14(b)] was investigated at a UV photolysis wavelength of 235 nm. The results of the

a)Author to whom correspondence should be addressed. Fax: +49-(0)6221-545050. Electronic mail: aw2@ix.urz.uni-heidelberg.de

latter studies demonstrated that vibrational excitation of the fundamental symmetric CH_3 ($1\nu_{CH}$) stretching mode leads to an increase in the chlorine-atom spin–orbit branching ratio compared to that of vibrationally unexcited CH_3CFCl_2 molecules.[14(a)] A comparable increase in the chlorine-atom spin–orbit branching ratio was observed in the 235 nm photolysis of CH_3CFCl_2 after preexcitation of the second ($3\nu_{CH}$) and third ($4\nu_{CH}$) overtones of the symmetric CH_3 stretching vibration, while at the same time the relative H atom versus chlorine atom product branching was found to decrease upon overtone excitation.[14(b)] However, to the best of our knowledge no measurements of absolute photoproduct quantum yields have been reported so far for the UV photodissociation of CH_3CFCl_2, which, along with the corresponding optical absorption cross sections,[8,9] are a prerequisite for a detailed understanding of its UV photochemistry in the atmosphere.

In the present article we report results of absolute chlorine and H atom quantum yield measurements in the 193.3 nm photolysis of CH_3CFCl_2, which were performed using the pulsed laser photolysis (LP)/VUV laser-induced fluorescence (LIF) ''pump-and-probe'' technique. In the present study, the nascent Cl-atom spin–orbit branching ratio, the absolute chlorine atom quantum yield Φ_{Cl+Cl^*}, and the absolute H atom quantum yield Φ_H were obtained by means of a photolytic calibration method employing HCl photolysis as a reference. In addition, the analysis of the measured Cl, Cl*, and H atom Doppler profiles along with *ab initio* calculations, carried out to determine the heat of formation of the CH_3CFCl_2 parent molecule and the CH_3CFCl radical, allowed us to derive information about the energy partitioning in the Cl, Cl*, and H atom forming photofragmentation step. Primary dissociation mechanisms for the formation of chlorine and H atoms will be discussed.

II. EXPERIMENT AND THEORETICAL CALCULATIONS

The present photodissociation experiments were carried out in a flow cell at mTorr level pressures using a LP/VUV-LIF pump-probe setup similar to the one previously used to study the chlorine and H atom formation dynamics in the UV photodissociation of CH_3CF_2Cl (HCFC-142b).[15,16]

CH_3CFCl_2 (ABCR-Chemicals, purity$>$99.7%) was pumped through the cell at room temperature. According to the manufacturer, the impurity consists of CH_3CF_2Cl and CH_3CF_3 (HFC-143a), with the latter compound having a negligible absorption at 193.3 nm. For CH_3CF_2Cl the room-temperature optical absorption cross section at 193.3 nm is $\sigma_{CH_3CF_2Cl}=0.58\times10^{-20}$ cm^2,[16,17] which is considerably lower than the corresponding absorption cross section of CH_3CFCl_2 ($\sigma_{CH_3CFCl_2}=5.58\times10^{-19}$ cm^2) recommended in Ref. 8(c). Because the impurity level is less than 0.3%, contributions from the photolysis of CH_3CF_2Cl can be neglected.

In the photodissociation experiments the CH_3CFCl_2 pressure in the cell was typically 9–23 mTorr: for the calibration measurements HCl (Messer Griesheim, 99.99%) was flowed through the reaction cell at pressures of typically 9–72 mTorr. The pressure in the cell was monitored by an MKS-Baratron. Flow rates were regulated by calibrated mass flow controllers and were maintained at high enough rates to ensure renewal of the gases between successive laser shots at a laser repetition rate of 6 Hz. The unpolarized output of an ArF excimer laser (193.3 nm emission wavelength, pulse duration 15–20 ns) was used as a ''pump'' laser to dissociate the CH_3CFCl_2 parent molecules as well as HCl. Pump laser intensities were typically between 2 and 10 mJ/cm^2.

For LIF detection of Cl, Cl*, and H atoms, narrow-band VUV ''probe'' laser radiation, tunable in the wavelength region 133.5–136.4 nm and around the H atom Lyman-α transition (121.567 nm) was generated by resonant third-order sum-difference frequency conversion ($\omega_{VUV}=2\omega_R-\omega_T$) of pulsed dye laser radiation (pulse duration 15–20 ns) in Kr and in a phase-matched Kr/Ar mixture, respectively.[18] In the four-wave mixing process the frequency ω_R ($\lambda_R=212.55$ nm) is two-photon resonant with the Kr $4p$-$5p$ (1/2, 0) transition. For chlorine atom LIF detection the second frequency ω_T could be tuned from 480 nm to 521 nm to cover the four allowed $Cl(4s^2P_{j'}\leftarrow3p^2P_{j''};\ j'=1/2,3/2\leftarrow j''=1/2,3/2)$ transitions.[19] Ground-state $Cl(^2P_{3/2})$ and excited-state $Cl^*(^2P_{1/2})$ atoms were detected via the ($j'=j''$) transitions, which have the highest transition probabilities $f_{3/2,3/2}=0.114$ and $f_{1/2,1/2}=0.088$, respectively.[20] For H atom LIF detection via the ($2p\ ^2P\leftarrow1s\ ^2S$) Lyman-α transition ω_T could be tuned from 844 to 846 nm. The fundamental laser radiation was obtained from two tunable dye lasers, simultaneously pumped by a XeCl excimer laser. The first dye laser was utilized to provide ω_T using Coumarin 307 dye in case of the Cl, Cl* LIF measurements and Styryl 9 dye for the H atom LIF detection. The second dye laser was operated with Coumarin 120 to generate light with a wavelength of 425.10 nm from which ω_R was obtained by frequency doubling with a BBO II crystal. The VUV light generated in the four-wave mixing process was carefully separated from the unconverted laser radiation by a lens monochromator followed by a light baffle system (for details see, e.g., Ref. 21). Maximum pulse energies up to 25 μJ can be achieved with this four-wave mixing method.[22] In the present study, however, the actual pulse energies were considerably lower due to absorption in the cell windows and optics. In all experiments the actual probe laser intensity was reduced until a linear intensity dependence of the LIF signal was obtained. The bandwidth [full width at half maximum (FWHM)] of the probe laser radiation was determined to be $\sim$0.3 cm^{-1} by measuring Doppler profiles of chlorine and H atoms generated in the 193.3 nm photolysis of HCl under thermalized conditions.

The probe beam was aligned to overlap the photolysis beam at right angles in the viewing region of a LIF detector. The delay time between the photolysis and probe laser pulses was controlled by a pulse generator and monitored on a fast oscilloscope. In the chlorine atom formation dynamics measurements, the delay time between pumping and probing was kept short enough, typically 80–150 ns (with a time jitter of about $\pm$10 ns), to allow the collision-free detection of the nascent Cl and Cl* atoms produced in the CH_3CFCl_2 and HCl photolysis. As outlined in Ref. 16, these delay times were chosen to avoid any time overlap between pump pulse

and probe laser pulse, which could results in unwanted multiphoton dissociation processes. Under the described experimental conditions, relaxation of Cl* by quenching as well as fly-out of Cl and Cl* atoms and secondary reactions with CH_3CFCl_2 and HCl were negligible.

In the H atom formation dynamics studies, the delay time between pumping and probing was kept at 80–100 ns. As in our previous CH_3CF_2Cl and HCl photolysis studies, the quality of the spatial overlap of the pump and the probe laser beam was carefully checked in order to ensure that no photolytically produced ''fast'' H atoms escape the detection region during the delay times used in the experiments (for details see Ref. 15).

Cl, Cl*, and H atom LIF signals were detected through bandpass filters, ARC model 130-B-1D, and 122-VN-1D, respectively, by a solar blind photomultiplier positioned at right angles to both pump and probe laser beams. The probe laser beam intensity was monitored after passing through the reaction cell. As the probe laser beam itself produced appreciable Cl, Cl*, and H atom LIF signals via photolysis of CH_3CFCl_2 and HCl, respectively, it was necessary to subtract these ''background'' atoms from the respective atoms produced in the 193.3 nm photolysis of CH_3CFCl_2 and HCl. Therefore, an electronically controlled mechanical shutter was inserted into the photolysis beam path, such that at each point of the fluorescence excitation spectra, the signal could first be 30 times averaged with the shutter opened and again be 30 times averaged with the shutter closed. Finally a point-by-point subtraction procedure was adopted[23] to obtain directly and on-line a LIF signal representing the contribution from Cl, Cl*, and H atoms generated solely by the 193.3 nm photolysis laser pulse. The LIF signals and the probe and photolysis laser intensity (the latter was monitored by a photodiode) were recorded with a boxcar system and transferred to a personal computer where the LIF signals were normalized to both pump and probe laser intensities. In the experiments special care was taken that the Cl, Cl*, and H atom signals generated by the 193.3 nm photolysis laser pulse showed a linear dependence on the pump (see, e.g., Fig. 1) and probe laser intensity.

In the present work the G2(MP2) method[24] of the GAUSSIAN 98 *ab initio* program package[25] was used for a direct calculation of heats of formation $\Delta_f H_{298}$ for the CH_3CFCl_2 parent molecule and for the CH_3CFCl fragment. For both species no experimental values are available. In case of CH_3CFCl_2 a value of $\Delta_f H^\circ_{298} = -335.1$ kJ/mol was reported in Ref. 26, which was estimated from available literature values of $\Delta_f H^\circ_{298}$ for CH_3CCl_3, CH_3CF_2Cl, and CH_3CF_3 employing a nonlinear fit procedure. The latter value was found to be in good agreement with the value $\Delta_f H^\circ_{298} = -333.3$ kJ/mol calculated by Melius with the BAC-MP4 method.[27] The value of $\Delta_f H^\circ_{298} = -358.6$ kJ/mol obtained for CH_3CFCl_2 in the present G2(MP2) calculations, however, deviates significantly from the results of the two previous calculations [for the CH_3CFCl radical the present G2(MP2) calculations yielded a value $\Delta_f H^\circ_{298} = -126.2$ kJ/mol]. Large deviations in the heats of formation of fluorinated and chlorinated compounds calculated by the G2(MP2) method were mentioned in Ref. 28 and attributed to systematic errors in the calculation of the atomization energies. It was found that the application of spin–orbit corrections can reduce the deviation from the experimental values in the case of chlorine compounds, and it was concluded that G2 theory is not sufficiently accurate for compounds containing two or more F and Cl atoms. However, the application of isodesmic reaction schemes, where the number of each kind of bond stays the same, was found to significantly improve the accuracy of the heats of formation values obtained by direct theoretical methods.[29] Therefore, G2(MP2) calculations on the isodesmic reaction scheme

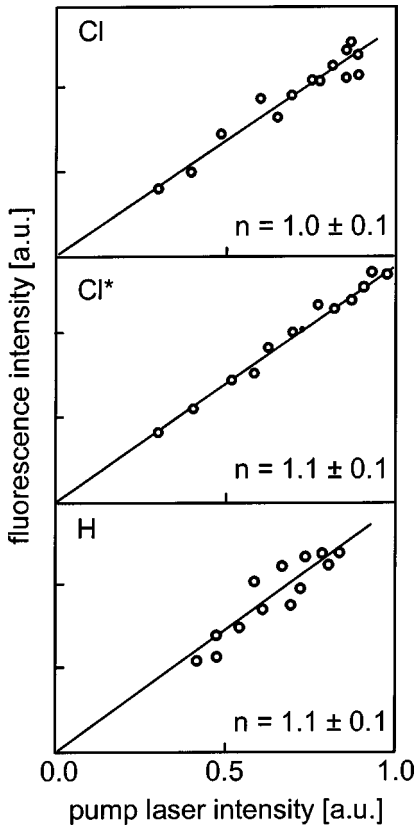

FIG. 1. Dependence of the observed Cl (a), Cl* (b), and H atom (c) LIF signal from the CH_3CFCl_2 photodissociation on the 193.3 nm photolysis (''pump'') laser intensity I_{pump}. Solid lines are the result of a least-squares fit (I^n_{pump}) to the experimental data in order to determine the power dependence n of the respective LIF signals. The values obtained for n are given in the figure.

$$CH_3CH_3 + CHFCl_2 \rightarrow CH_3CFCl_2 + CH_4 \quad (1)$$

were carried out in the present work to calculate the enthalpy change from which $\Delta_f H_{298}$ for CH_3CFCl_2 could be derived employing the literature values for the experimental heats of formation of CH_3CH_3 (-84.1 kJ/mol),[28] $CHFCl_2$ (-283.3 kJ/mol),[30] and CH_4 (-74.9 kJ/mol).[28] With this approach a value of $\Delta_f H^\circ_{298} = -339.2$ kJ/mol was obtained for CH_3CFCl_2, which is in reasonable agreement with the two values reported earlier.[26,27]

To derive an improved value for $\Delta_f H_{298}$ for CH_3CFCl a calculation on the isodesmic reaction

$$CH_3CH_2 + CHFCl_2 \rightarrow CH_3CFCl + CH_3Cl \quad (2)$$

TABLE I. Standard enthalpies of formation, $\Delta_f H^\circ_{298}$, and reaction enthalpies, $\Delta_r H^\circ_{298}$, of energetically accessible photochemical reaction channels R1–R14 in the 193.3 nm photolysis of CH_3CFCl_2. Energies available to the respective products, E_{avl}, were calculated via $E_{avl}=\hbar\omega_{pump}(193.3\text{ nm})-\Delta_r H^\circ_{298}$. Energies are given in kJ/mol.

Species	$\Delta_f H^\circ_{298}$	Ref.	Reaction channel	$\Delta_r H^\circ_{298}$	E_{avl}	
CH_3CFCl_2	−339.2	a	$CH_3CFCl_2\rightarrow CH_3CCl_2+F$	461.8	157.9	R1a
CH_3CFCl	−119.1	a	$CH_3CFCl_2\rightarrow CH_3CCl_2+F^*$	466.6	153.1	R1b
CH_3CCl_2	43.2	27	$CH_3CFCl_2\rightarrow CH_2CFCl_2+H$	449.0	170.7	R2
CH_2CFCl_2	−108.2	27	$CH_3CFCl_2\rightarrow CH_3CF+Cl_2$	407.1	212.6	R3
CH_2CFCl	−165.4	52	$CH_3CFCl_2\rightarrow CH_3CCl+ClF$	500.9	118.8	R4
CH_3CCl	212.0	53	$CH_3CFCl_2\rightarrow CH_2CFCl+HCl$	81.5	538.2	R5
CH_3CF	67.9	27	$CH_3CFCl_2\rightarrow CH_2CCl_2+HF$	69.0	550.7	R6
CH_2CCl_2	2.2	54	$CH_3CFCl_2\rightarrow CH_3+CFCl_2$	389.7	230.0	R7
CH_2CCl	257.0	27	$CH_3CFCl_2\rightarrow CH_2CCl+F+HCl$	583.3	36.4	R8a
CH_2CF	109.1	27	$CH_3CFCl_2\rightarrow CH_2CCl+F^*+HCl$	588.1	31.6	R8b
$CHCCl_2$	260.7	27	$CH_3CFCl_2\rightarrow CHCFCl+H+HCl$	542.7	77.0	R9
CHCFCl	77.8	a	$CH_3CFCl_2\rightarrow CHCCl_2+H+HF$	545.5	74.2	R10
$CFCl_2$	−95.2	27	$CH_3CFCl_2\rightarrow CH_2CF+Cl+HCl$	477.3	142.4	R11a
CH_3	145.7	31	$CH_3CFCl_2\rightarrow CH_2CF+Cl^*+HCl$	487.9	131.8	R11b
ClF	−50.3	31	$CH_3CFCl_2\rightarrow CH_3CFCl+Cl$	341.4	278.3	R12a
HCl	−92.3	31	$CH_3CFCl_2\rightarrow CH_3CFCl+Cl^*$	352.0	267.7	R12b
HF	−272.4	31	$CH_3CFCl_2\rightarrow CH_2CFCl+Cl+H$	513.1	106.6	R13a
F/F*	79.4/84.2	31	$CH_3CFCl_2\rightarrow CH_2CFCl+Cl^*+H$	523.7	96.0	R13b
Cl/Cl*	121.3/131.6	31	$CH_3CFCl_2\rightarrow CH_2CCl+Cl+HF$	445.1	174.6	R14a
H	218.0	31	$CH_3CFCl_2\rightarrow CH_2CCl+Cl^*+HF$	455.7	164.9	R14b

[a]values obtained in the present work from G2(MP2) calculations employing different isodesmic reaction schemes (details are given in the text).

was performed using the experimental heats of formation of CH_3CH_2 (120.9 kJ/mol),[28] $CHFCl_2$ (−283.3 kJ/mol),[30] and CH_3Cl (−83.7 kJ/mol).[30] The latter calculation yielded a value of $\Delta_f H^\circ_{298}=-119.1$ kJ/mol for the CH_3CFCl radical. The $\Delta_f H^\circ_{298}$ values obtained for CH_3CFCl_2 and CH_3CFCl via the isodesmic reactions (1) and (2), respectively, are listed in Table I along with available literature values of other possible photolysis products, which were used to calculate the reaction enthalpies $\Delta_r H^\circ_{298}$ of different dissociation channels and the corresponding values of the energies available to the products. With the $\Delta_f H^\circ_{298}$ values for CH_3CFCl_2 and CH_3CFCl of the present work along with the $\Delta_f H^\circ_{298}$ value reported in Ref. 31 for the Cl atom a value of $\Delta_r H^\circ_{298}=341.4$ kJ/mol for the C–Cl bond breaking reaction channel $CH_3CFCl_2\rightarrow CH_3CFCl+Cl$ can be obtained, which is in good agreement with an estimated value of 351 ±35 kJ/mol reported in Ref. 14(c).

In the same way, the heat of formation value $\Delta_f H_{298}=77.8$ kJ/mol for the CHCFCl radical, for which to the best of our knowledge also no experimental value is available, was calculated employing the isodesmic reaction scheme

$$CHCH_2+\tfrac{1}{4}CCl_4+\tfrac{1}{4}CF_4\rightarrow CHCFCl+\tfrac{1}{2}CH_4 \qquad (3)$$

along with the known heats of formation of $CHCH_2$ (299.6 kJ/mol),[27] CCl_4 (−95.8 kJ/mol), CF_4 (−993 kJ/mol), and CH_4 (−74.9 kJ/mol).[28]

III. RESULTS

A. [Cl*]/[Cl] spin–orbit branching ratio and primary quantum yields for chlorine and hydrogen atom formation

Primary quantum yields Φ_{Cl} for Cl and Φ_{Cl^*} for Cl* atom photofragment formation were measured separately by calibrating the Cl and Cl* atom signals $S_{Cl}(CH_3CFCl_2)$ and $S_{Cl^*}(CH_3CFCl_2)$ obtained in the CH_3CFCl_2 photodissociation against the Cl and Cl* atom signals $S_{Cl}(HCl)$ and $S_{Cl^*}(HCl)$ generated in the 193.3 nm photolysis of HCl (see Fig. 2). Values for the quantum yields Φ_{Cl} and Φ_{Cl^*} in the photolysis of CH_3CFCl_2 were determined using Eqs. (4a) and (4b), respectively,[16]

$$\Phi_{Cl}=\gamma_{Cl}\{S_{Cl}(CH_3CFCl_2)\,\phi_{Cl}\sigma_{HCl}p_{HCl}\}/\{S_{Cl}(HCl)\,\sigma_{CH_3CFCl_2}p_{CH_3CFCl_2}\}. \qquad (4a)$$

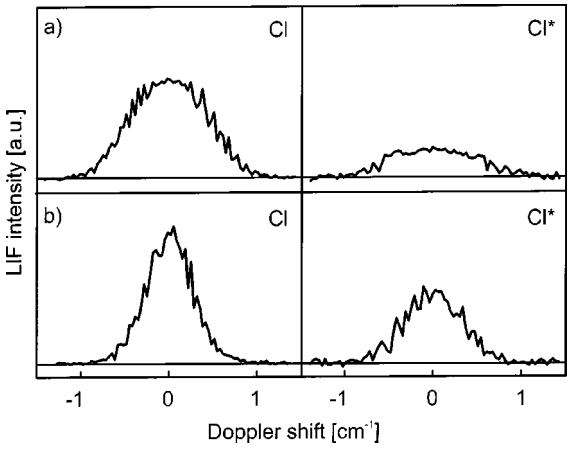

FIG. 2. Doppler profiles of Cl and Cl* (a) atoms produced in the 193.3 nm laser photolysis of 12 mTorr of CH_3CFCl_2 and Cl and Cl* (b) atoms produced in the 193.3 nm laser photolysis of 72 mTorr of HCl. Doppler profiles were recorded 150 ns after the photolysis laser pulse. Line centers correspond to the $(4s\,^2P_{j'=3/2}\leftarrow 3p\,^2P_{j''=3/2})$ transition of the Cl atom (74 225.8 cm^{-1}) and to the $(4s\,^2P_{j'=1/2}\leftarrow 3p\,^2P_{j''=1/2})$ transition of the Cl* atom (73 983.1 cm^{-1}), respectively.

$$\Phi_{Cl^*} = \gamma_{Cl^*}\{S_{Cl^*}(CH_3CFCl_2)\,\phi_{Cl^*}\sigma_{HCl}p_{HCl}\}/ \{S_{Cl^*}(HCl)\,\sigma_{CH_3CFCl_2}p_{CH_3CFCl_2}\}. \quad (4b)$$

σ_{HCl} and $\sigma_{CH_3CFCl_2}$ are the optical absorption cross sections of HCl and CH_3CFCl_2 at room temperature at 193.3 nm. S_{Cl} and S_{Cl^*} are the integrated areas under the measured Cl and Cl* atom Doppler profiles and p_{HCl} and $p_{CH_3CFCl_2}$ are the pressures of HCl and CH_3CFCl_2, respectively. $\phi_{Cl^*}=0.40$ and $\phi_{Cl}=0.60$ are the Cl and Cl* quantum yields in the 193.3 nm photolysis of HCl, which can be derived, because the photodissociation of HCl generates H+Cl(Cl*) products with a quantum yield of unity ($\phi_H=\phi_{Cl^*}+\phi_{Cl}=1$), from the [Cl*]/[Cl] spin–orbit branching ratio, 0.67 ± 0.09, reported in Ref. 16. For the HCl absorption cross section the value $\sigma_{HCl}=(8.1\pm0.4)\times10^{-20}$ cm^2 was used, which has been measured for the ArF excimer laser emission wavelength (193.3 nm).[32] The latter value is in good agreement with the value of 8.26×10^{-20} cm^2 obtained by nonlinear interpolation from the recommended data[8(b)] given in Ref. 33. For the CH_3CFCl_2 absorption cross section the value $\sigma_{CH_3CFCl_2}=(5.58\pm0.11)\times10^{-19}$ cm^2 derived from the data recommended in Ref. 8(c) was employed.

The factors γ_{Cl^*} and γ_{Cl} in Eqs. (4a) and (4b), respectively, are corrections accounting for the different degrees of absorption of the Cl ($\lambda_{probe}\approx134.72$ nm) and Cl*($\lambda_{probe}\approx135.16$ nm) VUV probe laser radiation by CH_3CFCl_2 and HCl. These absorption corrections were directly determined from the known distances inside the flow cell and the relative difference in the probe laser attenuation measured in the CH_3CFCl_2 and HCl photolysis runs. Under the present experimental conditions the absorption corrections were $\gamma_{Cl}=0.94\pm0.05$ and $\gamma_{Cl^*}=0.96\pm0.05$. The experimental data sets evaluated via Eqs. (4) to determine Φ_{Cl} and Φ_{Cl^*} consisted of 13 Cl (Cl*) atom profiles obtained in combination with 13 Cl (Cl*) profiles from HCl calibration runs. Experimental errors were determined from the 1σ statistical uncertainties of the experimental data, the uncertainties of the optical absorption cross sections, and the uncertainty of the [Cl*]/[Cl] branching ratio value in the 193.3 nm photolysis of HCl using simple error propagation. Values of $\Phi_{Cl}=0.74\pm0.11$ and $\Phi_{Cl^*}=0.27\pm0.03$ were obtained, resulting in a spin–orbit branching ratio of $[Cl^*]/[Cl]=\Phi_{Cl^*}/\Phi_{Cl}=0.36\pm0.08$. From the measured Cl and Cl* atom quantum yields a value of $\Phi_{Cl+Cl^*}=1.01\pm0.14$ can be derived for the total chlorine atom quantum yield in the 193.3 nm photolysis of CH_3CFCl_2.

The absolute primary quantum yield Φ_H for H atom formation in the CH_3CFCl_2 photodissociation was determined by calibrating the H atom signal obtained in the CH_3CFCl_2 photodissociation against the H atom signal measured in the 193.3 nm photolysis of HCl (see Fig. 3). As in the case of the chlorine atom quantum yield measurements, an absorption correction had to be applied to account for the difference in the absorption cross sections of CH_3CFCl_2 and HCl at the Lyman-α probe laser wavelength.[34] Under the present experimental conditions the absorption correction was $\gamma_H=0.85\pm0.04$. Further details about the calibration procedure are given in Ref. 15. For Φ_H a value of 0.04 ± 0.01 was obtained in the evaluation of eight independent calibration measurements.

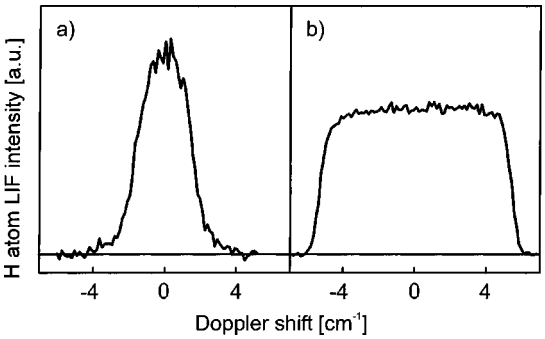

FIG. 3. Doppler profiles of H atoms produced in the 193.3 nm laser photolysis of (a) 8 mTorr of CH_3CFCl_2 and (b) 7 mTorr of HCl. Doppler profiles were recorded 100 ns after the photolysis laser pulse. Line centers correspond to the H atom Lyman-α transition (82259 cm^{-1}).

B. Average chlorine and hydrogen atom translational energies

Cl, Cl*, and H atom Doppler profiles were analyzed in order to determine the mean kinetic energy of the respective fragments in the photolysis of CH_3CFCl_2. The Doppler profiles directly reflect, via the linear Doppler shift $[\nu-\nu_0]/\nu_0=v_z/c$, the distribution $f(v_z)$ of the velocity component v_z of the absorbing atoms along the propagation direction of the probe laser beam. As a consequence, for an isotropic velocity distribution the average kinetic energy of the fragments in the laboratory system is given by $E_{T,lab}=\frac{3}{2}m\langle v_z^2\rangle$. Here $\langle v_z^2\rangle$ and m represent the second moment of the laboratory velocity distribution $f(v_z)$ and the mass of the photolytically produced atoms, respectively. However, because the measured spectral profiles represent a convolution of the laser spectral profile and the Doppler profile of the absorbing atoms, a numerical deconvolution was applied to obtain the correct fragment velocity distribution $f(v_z)$ employing a Gaussian function to describe the VUV probe laser spectral profile (for details see, e.g., Refs. 15 and 16).

In the chlorine atom formation dynamics studies the evaluation of the 26 recorded Cl and Cl* atom Doppler profiles, taking into account the actual laser bandwidth, yielded values of $E_{T,lab(Cl)}=107\pm8$ kJ/mol and $E_{T,lab(Cl^*)}=113\pm8$ kJ/mol for the mean laboratory kinetic energy of the respective fragments. For the H atoms produced in the CH_3CFCl_2 photolysis, a value of $E_{T,lab(H)}=25\pm4$ kJ/mol was obtained in the evaluation of the eight recorded Doppler profiles. The quoted errors include the 1σ statistical uncertainties obtained in the numerical least-squares fit analysis of the spectral profiles as well as the respective uncertainties of the laser bandwidth measurements. With the values given above the corresponding mean relative translational energies in the $CH_3CFCl+Cl$ center-of-mass system were calculated to be $E_{T(Cl)}=157\pm12$ kJ/mol and $E_{T(Cl^*)}=165\pm12$ kJ/mol.

IV. DISCUSSION

A. Primary quantum yield for chlorine atom formation

In principle, the amount of energy provided by a 193.3 nm photon ($\hbar\omega = 619.6$ kJ/mol) would be high enough to allow for a variety of two-body as well as three-body decay channels for the energized CH_3CFCl_2 molecule. The energetically allowed reaction product channels R1–R14 are listed in Table I. However, as absorption of a 193.3 nm photon actually leads to excitation in the first UV absorption band of CH_3CFCl_2, which originates from a $3p\pi \rightarrow \sigma^*$(C–Cl) transition within the valence shell ($3p\pi$ is a Cl lone pair orbital and σ^* is an antibonding C–Cl σ-MO), one can expect that UV photolysis leads preferentially to C–Cl bond breaking. The result of the present absolute quantum yield measurements for chlorine atom formation, $\Phi_{Cl+Cl^*} = 1.01 \pm 0.14$, is in line with this expectation. In addition, because the three-body decay channel in which two chlorine atoms are formed along with the CH_3CF radical is energetically not accessible in the 193.3 nm photolysis of CH_3CFCl_2, the result of the present chlorine atom quantum yield measurement can be directly used to derive an upper limit of $\Phi_{R1,\ldots,R10} \leqslant 0.13$ (Ref. 35) for the total quantum yield of the other thermochemically allowed two-body (R1–R7) and three-body (R8–R10) decay channels, which do not result in either Cl or Cl* atom formation (see Table I).

CH_3CFCl_2 pyrolysis experiments in which the thermal kinetics of the dehydrochlorination channel (R5) was studied in the temperature range 610–853 K yielded values of 196.6 kJ/mol (Ref. 36) and 238.7 kJ/mol (Ref. 37) for the activation energy of this channel. Only the latter value was found to be consistent with reaction threshold barrier energies of 225.9 and 236.0 kJ/mol obtained in chemical activation experiments[38] and *ab initio* quantum chemical calculations,[39] respectively. With an activation energy of 238.7 kJ/mol, the molecular elimination channel (R5) should be energetically accessible in the 193.3 nm photolysis of CH_3CFCl_2. However, the HCl($v = 0,1$) quantum yield of $\Phi_{HCl(v=0,1)} < 0.01$ reported in Ref. 13(a) along with the fact that no IR emission of HCl($v = 1-4$) could be observed following the 193.3 nm photolysis of CH_3CFCl_2 (Ref. 40) indicates that the HCl molecular elimination channel (R5) as well as HCl formation via the three-body decay channels (R8), (R9), and (R11) is only of minor importance in the primary UV photochemistry of CH_3CFCl_2. This parallels the results obtained in the UV photolysis of CH_3CH_2Cl where HCl elimination was also found to be a minor pathway only.[41] HCl formation observed in the 193.3 nm photodissociation of CH_3CH_2Cl was attributed to a mechanism, which involves internal conversion from the initially electronically excited state(s) to the electronic ground state. The fact that HCl could not be observed in case of CH_3CFCl_2 [Refs. 13(a) and 40] along with the quantum yield for chlorine atom formation of unity—as obtained in the present study—indicates that the dissociation takes place on one (or more) potential energy surface(s), which is (are) repulsive in the C–Cl coordinate and which is (are) not efficiently coupled to the $CH_3CFCl_2(A')$ electronic ground state.[13] In Ref. 14(c), based on the analysis of Cl and Cl* photofragment velocity distribution anisotropy parameters β measured in the 235 nm photolysis of CH_3CFCl_2 vibrationally preexcited to three and four quanta of C–H methyl stretches, it was proposed that electronically excited states of A' and A'' symmetry are involved in the UV photodissociation process for excitation energies up to 53 761 cm^{-1} (643.9 kJ/mol).

B. C–Cl bond cleavage mechanism, energy disposal, and [Cl*]/[Cl] spin–orbit branching ratio

Although the dynamics of C–Cl bond cleavage has been investigated previously for CH_3CFCl_2 under molecular beam conditions at photolysis wavelengths of 235 and 193.3 nm, no information about the energy disposal was derived in those studies.[13,14(a),14(b)] From the Cl and Cl* translational energies obtained in the present 193.3 nm photolysis study translational energy disposal fractions of $f_{T(Cl)} = E_{T(Cl)}/E_{avl} = 0.56$ and $f_{T(Cl^*)} = E_{T(Cl^*)}/E_{avl} = 0.62$, respectively, can be derived employing the respective values of E_{avl} for the two single Cl bond breaking reaction pathways,

$$CH_3CFCl_2 \rightarrow CH_3CFCl + Cl, \tag{R12a}$$

$$CH_3CFCl_2 \rightarrow CH_3CFCl + Cl^*, \tag{R12b}$$

as given in Table I. The present f_T values, which lie between the limiting values 0.36 and 0.85 predicted by a soft impulsive[42] and an impulsive rigid rotor model,[43] demonstrate that C–Cl bond cleavage leads to a rather high translational energy release in the CH_3CFCl_2 photodissociation. The present results therefore indicate the presence of a prompt dissociation from one or more PES's, which are strongly repulsive in the C–Cl coordinate. A prompt dissociation mechanism, which is consistent with the absence of any structure in the first absorption band of the CH_3CFCl_2 molecule, was also proposed in Ref. 14(c) to explain the nonvanishing Cl and Cl* photofragment velocity distribution anisotropy parameters β observed in the vibrationally mediated UV photodissociation of CH_3CFCl_2. The present results are in general agreement with the energy disposal fractions observed in the vibrationally mediated 235 nm photolysis of CH_3CFCl_2 ($3\nu_{CH}$), which, with a total excitation energy of 612.9 kJ/mol,[14(b)] is almost isoenergetic to the 193.3 nm ($\hbar\omega = 619.6$ kJ/mol) photolysis of vibrational ground-state CH_3CFCl_2. From the Cl and Cl* translational energies given in Ref. 14(a), values of $f_{T(Cl)} = 0.44$ and $f_{T(Cl^*)} = 0.51$ can be calculated using the thermochemical data of Table I. The fact that the latter values are somewhat smaller than the present values might be due to the absence of a significant energy flow from the initially excited C–H methyl stretch vibration into the C–Cl bond dissociation coordinate. In Ref. 14(c), the experimental observation that the Cl and Cl* product translational energies remained almost constant upon preexcitation with three, four, or even five quanta of C–H methyl stretch was attributed to the rather small amount of additional energy which finally ends up in the C–Cl coordinate after complete energy randomization among the 18 normal modes of the parent molecule. On the other hand, although C–H methyl stretch preexcitation was found to be insignificant for the energetics of Cl and Cl* atom formation, a pronounced influence on the overall Cl, Cl* signal strength and

on the [Cl*]/[Cl] spin–orbit branching ratio was observed.[13,14(a),14(b)] Upon vibrational excitation of the symmetric C–H methyl stretch vibration the spin–orbit branching ratio was observed to increase by about a factor of 2 from a value of $[Cl^*]/[Cl]=0.22\pm0.06$, as observed in the 193.3-nm ground-state photolysis of CH_3CFCl_2 under cold molecular beam conditions ($T_{vib}\approx100$ K),[13] to a value of $[Cl^*]/[Cl]=0.49\pm0.11$ in the isoenergetic 235 nm photolysis of CH_3CFCl_2 ($3\nu_{CH}$).[14(c)] In the present 193.3 nm gas-phase photolysis study of room-temperature CH_3CFCl_2 ($T=298$ K) an intermediate value of $[Cl^*]/[Cl]=0.36\pm0.08$ was obtained.

As has been suggested in Ref. 14(c), the alteration of the [Cl*]/[Cl] spin–orbit branching ratio upon vibrational preexcitation could be due to differences in the improvement of the Franck-Condon (FC) factors relative to the FC factors of the ground-state molecules. This is turn could result in an alteration of the ratio of the partial absorption cross sections to the upper electronically excited PES's (one of which has A' symmetry and correlates with Cl* fragments, and a second one with A'' symmetry which correlates with Cl fragments[13(c)]) involved in the dissociation process of the vibrationally excited molecules. In case that the [Cl*]/[Cl] spin–orbit branching ratio would indeed be determined by the relative strength of the two initial partial absorption cross sections, $\varepsilon^*(A'\rightarrow A')$ and $\varepsilon(A'\rightarrow A'')$ and not significantly altered by subsequent nonadiabatic interactions while the fragments separate, the higher [Cl*]/[Cl] spin–orbit branching ratio observed in the present 193.3-nm room-temperature photolysis study (compared to the 193.3 nm molecular beam photolysis study[13]) could be the result of the markedly different parent molecule vibrational state distributions. For the molecular beam conditions ($T_{vib}\approx100$ K) one can estimate that only a small fraction (ca. 7%) of the CH_3CFCl_2 molecules are in vibrational levels with $v>0$, while for the room temperature sample this value is considerably higher (ca. 78%).[44,45]

At this point, however, it should be noted that the observed dependence of the spin–orbit branching on C–H vibrational preexcitation[13,14] could also be due to the fact that (in the case that only one excited-state PES is involved in the UV dissociation process) different regions of the excited electronic state are sampled from which Cl and Cl* atom formation occurs via complex relaxation processes and conical intersections.

C. H atom formation dynamics

The H atom quantum yield of $\Phi_H=0.04\pm0.01$ obtained in the present work demonstrates that H atom formation, despite the fact that it could in principle occur via a number of reaction channels, such as (R2), (R9), and (R10), is only a minor product channel in the 193.3-nm gas-phase photolysis of CH_3CFCl_2. The rather low value of Φ_H along with the previously reported H atom quantum yields for CH_3CF_2Cl (Ref. 15), CH_3Cl, and CH_2Cl_2 (Ref. 46) show that photoabsorption at 193.3 nm, which leads to a $3p\pi\rightarrow\sigma^*$(C–Cl) valence shell transition,[47] does not result in efficient "primary" C–H bond cleavage.

In order to access whether "secondary" formation of H atoms via a three-body decay (denoted as R13 in Table I), which occurs most probably via a sequential mechanism

$$CH_3CFCl_2+\hbar\omega\rightarrow CH_3CFCl+Cl/Cl^*, \qquad \text{(R12a,b)}$$

followed by

$$CH_3CFCl\rightarrow CH_2CFCl+H, \qquad (5)$$

would be energetically possible in the 193.3 nm photolysis of CH_3CFCl_2, the kinetic energy distributions of the Cl and Cl* fragments derived from the Doppler profiles measured in the present study were analyzed employing the thermochemical data compiled in Table I. This analysis revealed that in the present case about 12% (corresponding to a fraction of 0.12) of the CH_3CFCl fragments formed in reactions (R12a,b) would have enough internal energy to further decompose via (5) into H atoms with an average relative translational energy of 25 ± 4 kJ/mol as observed in the present study and CH_2CFCl molecular fragments, if the latter are produced without internal excitation. The fact that the experimentally observed H versus chlorine atom formation ratio $[H]/[Cl+Cl^*]=\Phi_H/\Phi_{Cl+Cl^*}=0.04\pm0.02$ is about a factor of 3 lower might indicate that in the actual dissociation mechanism of the three-body decay channel (R13) the CH_2CFCl product fragments are formed with an significant amount of internal excitation.

Although the results of the energy analysis described above show that both the H atom translational energy and the H atom quantum yield of the present work would be consistent with the three-body decay (R13), the possibility that H atoms are formed to a certain extend via reaction channel (R2) or (R9) and (R10) cannot be completely ruled out on the basis of the present results. However, in any case an upper limit of $\Phi_{R2,R9,R10,R13}\leqslant0.05$ can be derived for the total yield of the H atom formation channels (R2), (R9), (R10), and (R13) from the upper error bound of the present H atom quantum yield measurement.

"Direct" H atom formation via reaction channel (R2) was proposed to explain the high average translation energy of 98 ± 19 kJ/mol, which was observed in the 193.3 nm CH_3CFCl_2 molecular beam laser photolysis studies along with a $[H]/[Cl+Cl^*]$ branching ratio of 0.18 ± 0.07.[13] For H atoms formed with an average translation energy of 98 kJ/mol, the kinetic energy distributions of the Cl, Cl* fragments as determined in the present work, assuming that under the molecular beam conditions of Ref. 13 the H and the chlorine atoms are formed through the reaction channel (R13), would only allow for a substantially smaller $[H]/[Cl+Cl^*]$ branching ratio of ca. 3×10^{-4} even in the limiting case of the CH_2CFCl molecular fragments being formed without any internal excitation. Therefore, it seems to be rather unlikely that the considerable amount of H atoms observed under molecular beam conditions can result from the three-body decay (R13). In addition, in case of the molecular beam photodissociation studies H atom formation along with HF formation through the three-body decay (R10) is also quite unlikely as for this product channel the amount of energy

available to the products, $E_{avl}=71.9$ kJ/mol, is considerably less than the observed average H atom product translational energy of 98 kJ/mol.

Therefore, the comparison between the present results obtained in a room-temperature photodissociation study and the results previously obtained under molecular beam conditions suggests that quite different H atom formation mechanisms are operating. While in the room-temperature photolysis relatively ''slow'' H atoms are formed most probably through a sequential three-body decay (R13), in which the H atoms originate from a ''secondary'' unimolecular decomposition of internally excited CH_3CFCl fragments produced in the ''primary'' C–Cl bond cleavage reaction (R12a,b), the ''fast'' H atom observed under ''cold'' molecular beam conditions are more likely to be formed by the two-body decay (R2) which involves single C–H bond cleavage. Furthermore, internal excitation of the parent molecule seems to have a pronounced influence on the [H]/[Cl+Cl*] branching ratio as indicated by the significant increase from a value of 0.04 ± 0.02 to a value of 0.18 ± 0.07, which is observed upon expansion cooling the parent molecule from room temperature down to a vibrational temperature of about 100 K. Results of [H]/[Cl+Cl*] branching ratio measurements obtained in the 235 nm molecular beam photolysis of vibrational ground-state and vibrationally preexcited CH_3CFCl_2, in which the [H]/[Cl+Cl*] branching ratio was found to decrease upon selective C–H methyl stretch excitation [see, e.g., the results obtained in the 235 nm photolysis of vibrational ground-state CH_3CFCl_2, $CH_3CFCl_2(3\nu_{CH})$, and $CH_3CFCl_2(4\nu_{CH})$ as reproduced in Table III of Ref. 14(b)], might be taken as an indication that the markedly different vibrational state distributions in the molecular beam and the room-temperature gas-phase experiments, which could result in a different Franck-Condon overlap between the ground vibronic and the electronically excited state wave functions, are the reason for the observed difference in the [H]/[Cl+Cl*] branching in the 193.3 nm photolysis. However, as already pointed out in Ref. 16 in conjunction with the interpretation of the 193.3 nm room-temperature and molecular beam photolysis results of CH_3CF_2Cl, additional theoretical work is clearly needed both on the involved electronically excited molecular PES' as well as on the molecular dissociation dynamics before it can be expected that a complete picture of the H atom formation mechanism(s) can be drawn for these molecules. On the experimental side, detailed information on the H atom energy release along with H atom photofragment velocity distribution anisotropy parameter measurements in particular in the vibrationally mediated CH_3CFCl_2 photolysis, for which the reported [H]/[Cl+Cl*] branching ratios indicate that H atom formation becomes a major product channel,[14(b),14(c)] would be most helpful to shed more light on the actual dissociation mechanism leading to H atom production.

D. HF formation

Preliminary studies of the 193.3-nm gas-phase photolysis of room-temperature CH_3CFCl_2, in which time-resolved Fourier-transform spectroscopy (TRFTS) in the emission mode was applied, indicated that vibrationally exited HF($v=1-5$) photofragments might be produced.[40] Based on the thermochemical data complied in Table I, HF could be formed in the 193.3 nm photolysis basically via the three-body decay channels (R10) and (R14), as well as via the unimolecular 1,2-elimination process (R6).[48]

Formation of HF($v=0,1$) via the three-body decay channel (R10) would be virtually consistent with the translational energy distribution derived from the H atom Doppler profiles measured in the present study. The analysis of the translational energy distribution revealed that HF($v=0$) formation is energetically possible for 98% of the experimentally observed H atoms. Formation of HF($v=1$) is still possible along with 52% of the observed H atom products. Formation of HF($v>1$), however, would energetically not be allowed. An upper limit of $\Phi_{R10}\leqslant 0.05$ for the quantum yield of HF molecules, which could be formed via reaction channel (R10), can be derived from the upper error bound of the H atom quantum yield measured in the present work.

The possibility for HF formation via the three-body decay channel (R14) can be assessed by analysing the translational energy distributions of the chlorine atom fragments observed in the present experiments. For this channel the analysis showed that HF($v=0$) formation is energetically possible along with up to 66% of the observed Cl and Cl* atoms. From the total chlorine atom quantum yield measured in the present work a value of $\Phi_{R14(HF)}=0.76$ can be obtained for the maximum quantum yield for HF($v=0$).[49] The analysis further revealed that only HF formation up to $v=3$ would be energetically allowed for reaction channel (R14). Hence it can be concluded that if HF($v>3$) products are observed, they must be formed via the elimination channel (R6). For the latter channel population of HF vibrational states up to $v=5$ as observed in Ref. 40 would be certainly possible considering the high value of the energy available to the products (see Table I).[50,51] Because reaction channel (R6) does not result in either Cl or Cl* fragments, the upper limit for the total quantum yield for HF formation via this channel is restricted by the relationship $\Phi_{R6}\leqslant\Phi_{R1,\ldots,R10}\leqslant 0.13$, which (*vide supra*) can be derived from the lower error bound of the present chlorine atom quantum yield measurement.[35]

From the above discussion it is clear that for a more quantitative assessment of the overall importance of HF formation in the UV photodissociation of CH_3CFCl_2 in general and the potential contributions of the three-body decay channels (R10, R14), in particular further experimental efforts toward the determination of the [HF($v=0$)]/[HF($v=1-5$)] branching ratio, which could not be provided by the TRFTS studies of Ref. 40, would be required.

V. SUMMARY

In the present gas-phase pulsed-laser photolysis and laser-induced fluorescence ''pump-and-probe'' experiments absolute quantum yields for photolytic formation of Cl, Cl*, and H atoms were determined after UV laser excitation of room-temperature CH_3CFCl_2 (HCFC-141b) at 193.3 nm. A value of $\Phi_{Cl+Cl*}=1.01\pm0.14$ was obtained for the total chlorine atom quantum yield along with a rather small H

atom quantum yield of $\Phi_H = 0.04 \pm 0.01$. These results demonstrate that chlorine atom formation is the main photochemical product channel in the 193.3-nm gas-phase photolysis of room-temperature CH_3CFCl_2. The fraction of the total available energy channeled into $CH_3CFCl + Cl/Cl^*$ product translational energy obtained in the present work was found to be in agreement with results of dynamical simulations in which repulsive models for single C–Cl bond cleavage were employed. The observed energy disposal along with the measured total chlorine atom quantum yield indicate that direct C–Cl bond cleavage on one or more repulsive PES' is the predominant primary fragmentation mechanism for CH_3CFCl_2 after photoexcitation in the first absorption band.

ACKNOWLEDGMENTS

The present work was partially supported by the Deutsche Forschungsgemeinschaft (DFG) via SFB 359 at the University Heidelberg. A.L. was supported by the Landesgraduierten Förderung Baden-Württemberg. D.S. wishes to acknowledge a postdoctoral fellowship provided by the DLR Bonn (Indo-German bilateral agreement, Project No. IND 99/050). H.R.V. would like to thank R. K. Vatsa and P. D. Naik (BARC, Mumbai, India) for many helpful discussions. J. Wolfrum (Director of the Institute of Physical Chemistry, Ruprecht-Karls-University Heidelberg) and J. P. Mittal (Director Chemistry Group, BARC, Mumbai, India) are thanked for their continuous support and interest in the ongoing work.

[1] E. Linak and P. Yau, *Chemical Economics Handbook* (SRI International, Menlo Park, CA, 1995).
[2] D. G. Gehring, D. J. Barsotti, and H. E. Gibbon, J. Chromatogr. Sci. **30**, 301 (1992).
[3] T. Shirai and Y. Makide, Chem. Lett. **4**, 357 (1998).
[4] *Scientific Assessment of Ozone Depletion: 1994*, World Meteorological Organization Report No. 37 (World Meteorological Organization, Geneva, Switzerland, 1995).
[5] Alternative Fluorocarbons Environmental Acceptability Study (AFEAS), "Product, and Sales of Fluorocarbons through 2000" (http://www.afeas.org/production and sales.html).
[6] See, e.g., R. P. Wayne, *The Chemistry of Atmospheres*, 2nd ed. (Oxford University Press, Oxford, 1991); R. Zellner, *Global Aspects of Atmospheric Chemistry* (Springer, New York, 1999) and references therein.
[7] (a) *ATLAS3 Public affairs status report #20*, NASA Science Operation Space Flight Center, Huntsville, 1994; (b) S. M. Schauffler, W. Pollock, E. L. Atlas, L. E. Heidt, and J. S. Daniel, Geophys. Res. Lett. **22**, 819 (1995); (c) J. M. Lee, W. T. Sturges, S. A. Penkett, D. E. Oram, U. Schmidt, A. Engel, and R. Bauer, *ibid.* **22**, 1369 (1995).
[8] (a) R. Warren, T. Gierczak, and A. R. Ravishankara, Chem. Phys. Lett. **183**, 403 (1991); (b) R. Atkinson, D. L. Baulch, R. A. Cox, R. F. Hampson, Jr., J. A. Kerr, M. J. Rossi, and J. Troe, J. Phys. Chem. Ref. Data **26**, 521 (1997); (c) W. B. DeMore, S. P. Sander, D. M. Golden, R. F. Hampson, M. J. Kurylo, C. J. Howard, A. R. Ravishankara, C. E. Kolb, and M. J. Molina, *Chemical kinetics and photochemical data for use in stratospheric modeling. Evaluation number 12*, JPL Publication **97-4**, 1 (1997), and references therein.
[9] A. Fahr, W. Braun, and M. J. Kurylo, J. Geophys. Res. **98**, 20467 (1993).
[10] R. Talukdar, A. Mellouki, T. Gierczak, J. B. Burkholder, S. A. McKeen, and A. R. Ravishankara, J. Phys. Chem. **95**, 5815 (1991).
[11] R. Warren, T. Gierczak, and A. R. Ravishankara, Chem. Phys. Lett. **183**, 403 (1991).
[12] T. J. Wallington and M. D. Hurley, Chem. Phys. Lett. **189**, 437 (1992); J. P. Sawerysyn, A. Talhaoui, B. Meriaux, and P. Devolder, Chem. Phys. Lett. **198**, 197 (1992); A. Talhaoui, F. Louis, P. Devolder, B. Meriaux, J.-P. Sawerysyn, M.-T. Rayez, and J.-C. Rayez, J. Phys. Chem. **100**, 13531 (1996).
[13] (a) A. Melchior, I. Bar, and S. Rosenwaks, J. Chem. Phys. **107**, 8476 (1997); (b) A. Melchior, H. M. Lambert, P. J. Dagdigian, I. Bar, and S. Rosenwaks, Isr. J. Chem. **37**, 455 (1997); (c) A. Melchior, Ph.D. thesis, Ben-Gurion University, Beer-Sheva, Israel, 2000.
[14] (a) A. Melchior, X. Chen, I. Bar, and S. Rosenwaks, Chem. Phys. Lett. **315**, 421 (1999); J. Chem. Phys. **112**, 10787 (2000); (c) T. Einfeld, C. Maul, K. H. Gericke, R. Marom, S. Rosenwaks, and I. Bar, *ibid.* **115**, 6418 (2001).
[15] R. A. Brownsword, M. Hillenkamp, T. Laurent, H.-R. Volpp, J. Wolfrum, R. K. Vatsa, and H.-S. Yoo, J. Chem. Phys. **107**, 779 (1997).
[16] R. A. Brownsword, P. Schmiechen, H.-R. Volpp, H. P. Upadhyaya, Y. J. Jung, and K.-H. Jung, J. Chem. Phys. **110**, 11823 (1999).
[17] A. F. Nayak, T. J. Buckley, M. J. Kurylo, and A. Fahr, J. Geophys. Res. **101**, 9055 (1996).
[18] G. Hilber, A. Lago, and R. Wallenstein, J. Opt. Soc. Am. B **4**, 1753 (1987).
[19] K. Tonokura, Y. Matsumi, M. Kawasaki, S. Tasaki, and R. Bersohn, J. Chem. Phys. **97**, 8210 (1992), and references therein.
[20] W. L. Wiese, M. W. Smith, and B. M. Miles, *Atomic Transition Probabilities*, Natl. Bur. Stand. Ref. Data Ser., Natl. Bur. Stand. (U.S.) Circ. No. 22 (U.S. GPO, Washington, D.C., 1969).
[21] R. A. Brownsword, C. Kappel, P. Schmiechen, H. P. Upadhyaya, and H.-R. Volpp, Chem. Phys. Lett. **289**, 241 (1998).
[22] J. P. Marangos, N. Shen, H. Ma, M. H. R. Hutchison, and J. P. Connerade, J. Opt. Soc. Am. B **7**, 1254 (1990).
[23] See e.g. R. A. Brownsword, M. Hillenkamp, T. Laurent, R. K. Vatsa, H.-R. Volpp, and J. Wolfrum, J. Chem. Phys. **106**, 1359 (1997).
[24] L. A. Curtiss, K. Raghavachari, and J. A. Pople, J. Chem. Phys. **98**, 1293 (1993).
[25] M. J. Frisch, G. W. Trucks, H. B. Schlegel *et al.* GAUSSIAN 98 Revision A.7, Gaussian, Inc., Pittsburgh, PA, 1998.
[26] S.-Y. Chiang, Y.-C. Lee, and Y.-P. Lee, J. Phys. Chem. A **105**, 1226 (2001).
[27] C. F. Melius, Sandia National Laboratories, BAC-MP4 heats of formation data file (version 6 July 1996).
[28] L. A. Curtiss, K. Raghavachari, P. C. Redfern, and J. A. Pople, J. Chem. Phys. **106**, 1063 (1997).
[29] R. J. Berry, D. R. F. Burgess Jr., M. R. Nyden, M. R. Zachariah, and M. Schwartz, J. Phys. Chem. **100**, 1984 (1996).
[30] R. J. Berry, D. R. F. Burgess, Jr., M. R. Nyden, M. R. Zachariah, C. F. Melius, and M. Schwartz, J. Phys. Chem. **100**, 7405 (1996), and references therein.
[31] M. W. Chase, Jr., J. Phys. Chem. Ref. Data Monogr. **9**, 1 (1998).
[32] Y. Mo, K. Tonokura, Y. Matsumi, M. Kawasaki, T. Sato, T. Arikawa, P. T. A. Reilly, Y. Xie, Y. Yang, Y. Huang, and R. J. Gordon, J. Chem. Phys. **97**, 4815 (1992).
[33] E. C. Y. Inn, J. Atmos. Sci. **32**, 2375 (1975).
[34] R. K. Vatsa and H.-R. Volpp, Chem. Phys. Lett. **340**, 289 (2001).
[35] The upper limit for the total quantum yield of the decay channels (R1–R10), which do not result in Cl and Cl* formation, is given by $1 - \Phi_{Cl+Cl^*}$ where Φ_{Cl+Cl^*} represents the lower error bound of the present chlorine atom quantum yield measurement ($\Phi_{Cl+Cl^*} = 0.87$).
[36] D. Sianesi, G. Nelli, and R. Fontanelli, Chim. Ind. (Milan) **50**, 619 (1968).
[37] G. Huybrechts and K. Eerdekens, Int. J. Chem. Kinet. **33**, 191 (2001).
[38] J. B. McDoniel and B. E. Holmes, J. Phys. Chem. **100**, 3044 (1996).
[39] J. L. Toto, G. O. Prichard, and B. Kirtman, J. Phys. Chem. **98**, 8359 (1994).
[40] S.-R. Lin, Y.-J. Chen, S.-C. Lin, and Y. P. Lee, in Proceedings of Trombay Symposium on Radiation and Photochemistry, 2000, pp. 315–326.
[41] M. Kawasaki, K. Kasatani, H. Sato, H. Shinohara, and N. Nishi, Chem. Phys. **88**, 135 (1984).
[42] A. F. Tuck, J. Chem. Soc., Faraday Trans. 2 **73**, 689 (1977).
[43] M. Kawasaki, K. Suto, Y. Sato, Y. Matsumi, and R. Bersohn, J. Phys. Chem. **100**, 19853 (1996).
[44] J. R. Durig, C. J. Wurrey, W. E. Bucy, and A. E. Sloan, Spectrochim. Acta, Part A **32**, 175 (1976).
[45] The relative population of the vibrationally excited states was estimated treating the CH_3CFCl_2 molecule as a quantum mechanical harmonic oscillator with 18 normal modes of vibration. The values for the respective vibrational frequencies were taken from Ref. 44.
[46] R. A. Brownsword, M. Hillenkamp, T. Laurent, R. K. Vatsa, H.-R. Volpp, and J. Wolfrum, J. Phys. Chem. A **101**, 5222 (1997).

[47] M. B. Robin, *Higher Excited States of Polyatomic Molecules* (Academic Press, New York, 1974), Vol. I.
[48] HF formation via reaction channel (R6) was observed in chemical activation experiments in which internally excited CH_3CFCl_2 molecules were formed by the recombination of CH_3 and $CFCl_2$ radicals (Ref. 38). In the latter study, a reaction threshold barrier energy of 284.5 kJ/mol was determined: however, no information regarding the HF product vibrational state distribution in the unimolecular 1,2-elimination process could be obtained.
[49] The upper limit for $\Phi_{R14(HF)}$, the quantum yield for HF formation through reaction channel (R14), was calculated via $\Phi_{R14(HF)}=0.66\times\overline{\Phi}_{Cl+Cl^*}=0.76$, where $\overline{\Phi}_{Cl+Cl^*}$ represents the upper error bound of the present chlorine atom quantum yield measurement ($\overline{\Phi}_{Cl+Cl^*}=1.15$). The value 0.66 represents the fraction of the Cl and Cl* atoms which can be formed along with HF($v=0$).
[50] Formation of HF up to $v=5$ was previously observed in the 193.3 nm photolysis of CH_2CF_2 [Ref. 51(a)] and CH_2CFCl [Ref. 51(b)] where the amount of energy available to the products of the respective HF elimination channels are comparable to that of the HF elimination channel (R6) in the 193.3 nm photolysis of CH_3CFCl_2.
[51] (a) G. E. Hall, J. T. Muckerman, J. M. Preses, R. E. Weston, Jr., G. W. Flynn, and A. Persky, J. Chem. Phys. **101**, 3679 (1994); (b) T. R. Fletcher and S. R. Leone, *ibid.* **88**, 4720 (1988).
[52] I. Barin, *Thermochemical Data for Pure Substances* (VCH, Weinheim, 1995).
[53] J. A. LaVilla and J. L. Goodman, J. Am. Chem. Soc. **111**, 6877 (1989).
[54] M. Mansson, B. Ringner, and S. Sunner, J. Chem. Thermodyn. **3**, 547 (1971).